# Tilt anisoplanatism and PSF retrieval in LGS MCAO using a predictive controller

R. Flicker[a,b] and F. Rigaut[b]

Gemini Preprint #70

a. Lund Observatory, Box 43, SE-22100 Lund, Sweden
b. Gemini Observatory, 670 N. A'ohoku Place, Hilo HI 96720 USA

# Tilt anisoplanatism and PSF retrieval in LGS MCAO using a predictive controller

Ralf Flicker[a b] and François Rigaut[b]

[a]Lund Observatory, Box 43, SE-22100 Lund, Sweden
[b]Gemini Observatory, 670 N. A'Ohoku Pl., HI-96720 Hilo, USA

## ABSTRACT

It is shown how Strehl ratio degradation due to tilt anisoplanatism in laser guide star supported multi-conjugated adaptive optics systems can be predicted by analytical models. Long exposure PSFs are retrieved from the model, and the advantage of implementing a predictive temporal controller to compensate for loop delay is demonstrated.

## 1. INTRODUCTION

The tip and tilt determination problem[1] associated with laser guide stars (LGS) was recognized in the early 90s (Rigaut & Gendron, 1992), and it was realized that an additional natural guide star (NGS) was required to obtain the global image motion. A new class of problems arise, however, when multiple LGS are employed to do tomography. The problem was observed in calculations by Ellerbroek in 1994, but not fully understood until recently (Ellerbroek & Rigaut, 2001, submitted): as a consequence of the tilt filtering, the high-order LGS system looses all tomographic information about the altitudes of the quadratic modes (one focus and two astigmatisms). If not amended, this would result in an incomplete tomographic reconstruction with a non-optimal compensation as a result.

The problem is straightforward and easily visualized by considering, for instance, a focus mode $Z_4(x,y) = 2\sqrt{3}(x^2+y^2)-\sqrt{3}$ centered on the optical axis at an altitude $h$. On looking an angle $\alpha$ to the side in the $x$-direction, one would measure $Z_4(x-h\alpha,y) = 2\sqrt{3}(x^2+y^2)-4\sqrt{3}xh\alpha+\sqrt{3}(h^2\alpha^2-1)$, which is the same amount of focus, some more piston and an additional linear term. Since the WFS is insensitive to piston, all information about the altitude of the mode is contained within the linear term. Because this is the term filtered from the LGS measurements, however, tomography fails, and the system does not know where to assign the focus correction. It is also possible for an altitude-conjugated quadratic mode to be partially canceled by an identical mode of opposite sign at ground level, leaving only tilts and pistons. In this case, the LGS system measures nothing at all, so these particular combinations form three additional null-modes (belonging to the null space of the LGS interaction matrix). These three, unlike global tip and tilt, are pure plate scale modes defined as the combinations $Z_i(\mathbf{x};h)-Z_i(\mathbf{x};h=0)$ for $i=4,5,6$. Both the failure of tomography on the quadratic modes and the presence of pure plate scale modes in the atmosphere will cause tilt anisoplanatism if not compensated.

The obvious solution to this would be to either shift the measurement of quadratic modes to the NGS, with some penalty in limiting magnitude, or to employ multiple tip/tilt NGS measuring the differential tilt over the field. As there are now five null-modes, one would for the latter scenario require at least three NGS (six measurements) to obtain an over-determined problem to solve. It will be shown in the following analysis that one deformable mirror (DM) conjugated to a non-zero altitude would be able to perfectly correct tilt anisoplanatism up to noise, aliasing and servo lag.

## 2. MODAL ANALYSIS

Adopting the Taylor hypothesis and the near-field approximation, we model the turbulence as a set of discrete layers and the propagation of light as geometric phase additivity. The open loop phase $\varphi$ in the plane of the telescope pupil expanded on the five first Zernikes may be then written

$$\varphi(\mathbf{x},\boldsymbol{\theta},t) = \sum_{l=0}^{N_l}\varphi_l(\mathbf{x}+h_l\boldsymbol{\theta},t) = \sum_{l=0}^{N_l}\sum_{i=2}^{6} a_{il}(t)\,Z_i\left[(\mathbf{x}+h_l\boldsymbol{\theta})/R_l\right], \quad (1)$$

E-mail: ralf@astro.lu.se, frigaut@gemini.edu

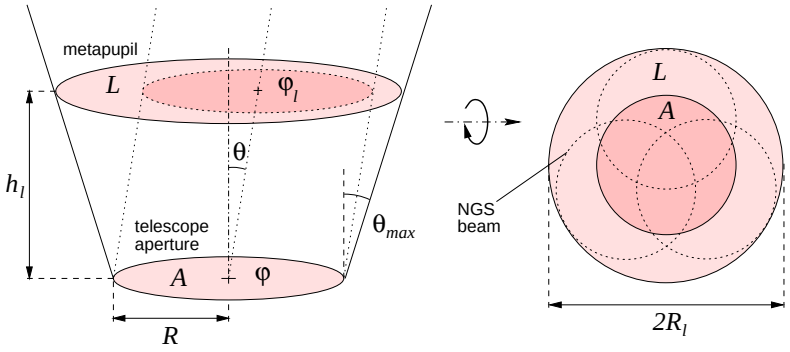


**Figure 1.** Left: geometry and notation for phase projection onto the telescope aperture $\mathcal{A}$ through discrete turbulent layers as in the Taylor hypothesis. Right: example of three NGS beam-prints defining the meta-pupil $\mathcal{L}$.

where $N_l$ is the number of turbulent layers and $a_{il}$ is the time dependent expansion coefficient pertaining to Zernike mode $Z_i$ and turbulence layer $l$. If $R$ is the telescope aperture radius, $h_l$ the altitude of layer $l$ and $\theta_{max}$ the largest angle subtended by the NGS, the radii of the meta-pupils (*cf.* figure 1) over which the Zernikes are defined are $R_l = R + h_l\theta_{max}$. On introducing the Zernikes in Cartesian coordinates and expanding, one will obtain terms which are constant, linear and quadratic in $x$ and $y$. The constant terms (piston) are discarded as they do not affect image quality, and the quadratic terms are assumed to be sensed and corrected by the high-order MCAO system. The remaining linear terms $\varphi_\pi$ may be written as a field-dependent linear combination of tip and tilt over the telescope aperture

$$\varphi_\pi(\mathbf{x},\boldsymbol{\theta},t) = \sum_{i=2}^{6} A_i(t)[c_{i2}(\boldsymbol{\theta})Z_2(x/R) + c_{i3}(\boldsymbol{\theta})Z_3(y/R)], \tag{2}$$

where the coefficients $\mathbf{c}_2$ and $\mathbf{c}_3$ are found to be

$$\mathbf{c}_2(\boldsymbol{\theta}) = [1, 0, 2\sqrt{3}\theta_x, \sqrt{6}\theta_y, \sqrt{6}\theta_x] \tag{3}$$

$$\mathbf{c}_3(\boldsymbol{\theta}) = [0, 1, 2\sqrt{3}\theta_y, \sqrt{6}\theta_x, -\sqrt{6}\theta_y], \tag{4}$$

and the notation

$$A_{[2,3]}(t) = \sum_{l=0}^{N_l} a_{[2,3]l}(t)R/R_l \quad \text{and} \quad A_{[4:6]}(t) = \sum_{l=0}^{N_l} a_{[4:6]l}(t)h_l R/R_l^2 \tag{5}$$

was introduced. Consider now an MCAO system that has one DM conjugated to a non-zero altitude $h_M$ and one conjugated to zero, capable of producing (at least) Zernikes up to $Z_6$. Expanding the DM phase on the basis $\alpha$, it becomes a matter of straightforward algebra to show that the residual compensated phase $\varphi_c$ can be written as a linear combination of tip and tilt like

$$\varphi_c(\mathbf{x},\boldsymbol{\theta},t) = \sum_{k=2}^{3} \gamma_k(\boldsymbol{\theta},t)Z_k(\mathbf{x}/R), \tag{6}$$

where the time and field dependent tip and tilt coefficients $\gamma_k$ are

$$\gamma_k(\boldsymbol{\theta},t) = \sum_{i=2}^{6} c_{ik}(\boldsymbol{\theta})[A_i(t) - w_i\alpha_i(t)], \quad k = 2,3; \quad w_i = \begin{cases} 1, & i = 2,3 \\ h_M/R, & i = 4,5,6\,. \end{cases} \tag{7}$$

## 3. SYSTEM LOOP DYNAMICS

Central to the analysis is the temporal dynamics of the system, since the performance is chiefly a servo-lag/noise trade-off. Referring to the block diagram in figure 2, the open loop transfer function $\mathcal{H}$ is

$$\mathcal{H}(f) = \left.\frac{\widetilde{\alpha}(f)}{\widetilde{a}(f)}\right|_{ol} = \mathcal{S}(f)\mathcal{R}(f)\mathcal{C}(f)\mathcal{D}(f), \tag{8}$$

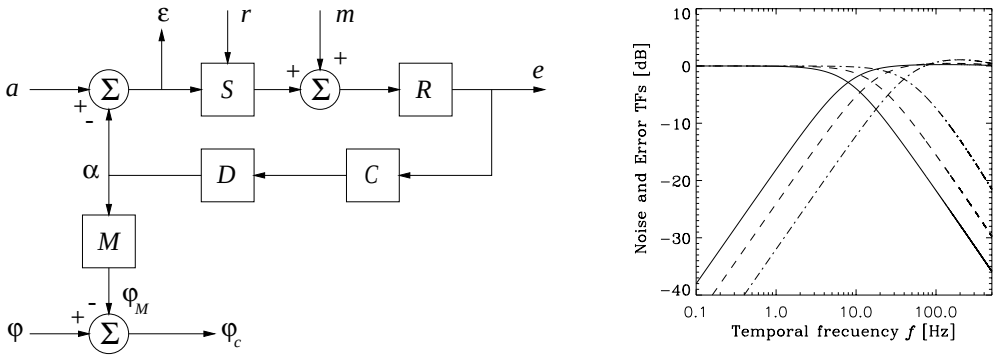


**Figure 2.** Left: simplified block diagram of temporal control loop. Right: examples of attenuation by $\mathcal{H}_n$ and $\mathcal{H}_\varepsilon$ for three values of the gain: $g = 0.05$ (solid), $g = 0.1$ (dashed), $g = 0.25$ (dot-dashed).

where the component transfer functions in Fourier space are given by

$$\mathcal{S}(f) = \mathrm{sinc}(f/f_s)\exp(-i\pi f/f_s)\ , \quad \text{sensor} \tag{9}$$

$$\mathcal{R}(f) = \exp(-2\pi i f\tau)\ , \quad \text{reconstructor} \tag{10}$$

$$\mathcal{C}(f) = \text{compensator (to be optimized)} \tag{11}$$

$$\left\{\text{simple integrator} = \frac{g_i f_s}{2\pi i f}\right\} \tag{12}$$

$$\mathcal{D}(f) = \exp(-i\pi f/f_s)\ , \quad \text{DAC}, \tag{13}$$

and $f_s$ is the sampling frequency. For the present null-mode analysis we can safely omit aliasing contribution from uncompensated modes, which is deemed to be small, as the LGS system compensates many modes above the null-modes. Folding in the temporal response of the system, the estimated modal commands in frequency domain are then given by

$$\widetilde{\widehat{\alpha}}_i = \widetilde{A}_i \mathcal{H}_{cl}(g_i)/w_i + \widetilde{n}_i \mathcal{H}_n(g_i). \tag{14}$$

$\mathcal{H}_{cl}$ and $\mathcal{H}_n$ are the closed loop and noise transfer functions, given by

$$\mathcal{H}_{cl} = \frac{\mathcal{H}}{1+\mathcal{H}} \quad \text{and} \quad \mathcal{H}_n = \frac{\mathcal{R}\mathcal{C}}{1+\mathcal{H}}. \tag{15}$$

Some examples of $\mathcal{H}_n$ and the error transfer function $\mathcal{H}_\varepsilon = \mathcal{H}_{cl}/\mathcal{H}$ for different values of the gain $g$ are plotted in figure 2, for $t_i = 1$ ms and $\tau = 0.1$ ms.

### 3.1. Predictive controller

As the linear and quadratic modes of the atmosphere are relatively slow compared to the bandwidth of the system, a predictive temporal controller (henceforth *predictor*) may be able to improve performance by compensating for the delay in the loop. Several adaptive schemes have been proposed that either attempt to adaptively update the reconstruction matrix (*e.g.* Ellerbroek & Rhodarmer, 2001)[2] the controller parameters (*e.g.* Dessenne *et al.*, 1998),[3] or both. The adaptive predictor algorithm of (Dessenne *et al.*, 1998) has the analytical advantage that the error minimization criterion can be expressed in terms of constraints on the transfer functions, which enables us to incorporate some aspects of this method directly into our analysis. This ideal predictor $\mathcal{C}(f)$ should be of the form

$$\|\mathcal{C}(f, g_i)\|^2 = \frac{\Phi_i(f)}{C_n^{ii}}, \quad \forall f, \tag{16}$$

which states that $\|\mathcal{C}_i\|^2$ should be an estimation of the spectral SNR of the input turbulent mode $a_i(t)$. While this information is of little use in practice (the optimization algorithm can not access $a_i$), it does allow us to test the

ideal predictor in the present tilt anisoplanatism analysis as a first step. In the loop, the linear controller described in $\mathcal{Z}$-domain by

$$\mathcal{C}(z = e^{2\pi i f}) = \frac{\sum_{l=0}^{q-1} a_l z^{-l}}{1 + \sum_{l=1}^{p-1} b_l z^{-l}} \tag{17}$$

has it's parameters $\{a_l\}_{l=0}^{q-1}$ and $\{b_l\}_{l=1}^{p-1}$ adaptively updated according to the prescribed algorithm.[3] It is the task of the algorithm to tune these parameters to make $\mathcal{C}$ as close as possible to $\Phi/C_n$. For stability reasons, the optimal predictor can in practice not be arbitrarily close to the ideal. For the low-order null-mode loop we are considering, however, stability constraints will not impinge heavily on the optimal performance for the range of modal gains likely to be used. Hence an optimal linear predictor of this kind may perform close to the ideal in the case of this null-mode system.

## 4. TILT ANISOPLANATISM COVARIANCE MATRIX

As will be shown in the next section, the covariance matrix $C_\gamma = \langle \gamma\gamma^T \rangle$ allows us to compute the Strehl ratio due to tilt anisoplanatism and reconstruct the corresponding PSF. Referring to the notation in figure 2, one may eliminate $\alpha$ in favor of $n$ in the above expression to arrive at the following expression for the covariances

$$C_\gamma^{kl}(\boldsymbol{\theta}) = \sum_{i,j=2}^{6} c_{ik}(\boldsymbol{\theta}) c_{il}(\boldsymbol{\theta}) [\mathcal{E}_{ij} + w_i w_j \mathcal{N}_{ij}], \tag{18}$$

where the servo-lag $\mathcal{E}$ and noise $\mathcal{N}$ terms are given by

$$\mathcal{E}_{ij} = 2 \times \int_0^{f_s} df \, \mathrm{Re}\left[\Phi_{ij}(f) \mathcal{H}_\varepsilon(f, g_i) \mathcal{H}_\varepsilon^*(f, g_j)\right], \tag{19}$$

$$\mathcal{N}_{ij} = C_n^{ij} \frac{1}{2 f_s} \int_{-f_s}^{+f_s} df \, \mathcal{H}_n(f, g_i) \mathcal{H}_n^*(f, g_j). \tag{20}$$

The error and noise transfer functions $\mathcal{H}_\varepsilon$ and $\mathcal{H}_n$ were defined in section 3, and $\Phi$ is the temporal Zernike power spectrum in Kolmogorov turbulence. Assuming a single wind direction, it was computed as in (Roddier *et al.*, 1993),[4] but more complicated geometries are treated in (Whitely *et al.*, 1998).[5] The modal noise covariance matrix is $C_n = E\langle \mathbf{m}\mathbf{m}^T \rangle_t E^T$, where $E$ is the null-mode reconstruction matrix.

## 5. STREHL PREDICTION AND PSF RETRIEVAL

To arrive at a PSF estimate, (Véran *et al.*, 1997)[6] derives a procedure to compute the pupil-averaged phase structure function $\bar{D}_{\varphi_c}(\boldsymbol{\rho}, \boldsymbol{\theta})$ from $C_\gamma(\boldsymbol{\theta})$. In the near field approximation, the long exposure optical transfer function $B(\boldsymbol{\rho}/\lambda, \boldsymbol{\theta})$ is then simply

$$B(\boldsymbol{\rho}/\lambda, \boldsymbol{\theta}) = (P \star P) e^{-\frac{1}{2}\bar{D}_{\varphi_c}(\boldsymbol{\rho}, \boldsymbol{\theta})} = B_{tel}(\boldsymbol{\rho}/\lambda) B_\gamma(\boldsymbol{\rho}/\lambda, \boldsymbol{\theta}), \tag{21}$$

where $\star$ denotes autocorrelation, and the PSF is obtained by Fourier transform. The pupil-averaging approximation

$$\bar{D}_{\varphi_c}(\boldsymbol{\rho}) = \frac{\int_{-\infty}^{+\infty} d\mathbf{x} \, P(\mathbf{x}) P(\mathbf{x} + \boldsymbol{\rho}) D_{\varphi_c}(\mathbf{x}, \boldsymbol{\rho})}{\int_{-\infty}^{+\infty} d\mathbf{x} \, P(\mathbf{x}) P(\mathbf{x} + \boldsymbol{\rho})} \tag{22}$$

will in fact be perfectly valid in this special case where the errors are all tilts. Inserting (6) into the definition of $D_{\varphi_c}$ leads to the following quadratic form for the pupil averaged structure function

$$\bar{D}_{\varphi_c}(\boldsymbol{\rho}) = R^{-2} \left[ C_\gamma^{22} \rho_x^2 + C_\gamma^{33} \rho_y^2 + 2 C_\gamma^{23} \rho_x \rho_y \right]. \tag{23}$$

Since the tilt anisoplanatism OTF $B_\gamma \equiv \exp(-\frac{1}{2}\bar{D}_{\varphi_c})$ is the negative exponential of a quadratic form, it's shape is a rotated Gaussian. In a transformed coordinate system $\boldsymbol{\rho}' = T\boldsymbol{\rho}$, where $T$ is a rotation about the origin, it will become a pure Gaussian. In this rotated basis, an exact expression for the Strehl ratio that foregoes PSF reconstruction is given by

$$SR = \sqrt{\frac{1}{1 + 2C_\gamma^{22}}} \times \sqrt{\frac{1}{1 + 2C_\gamma^{33}}}. \tag{24}$$

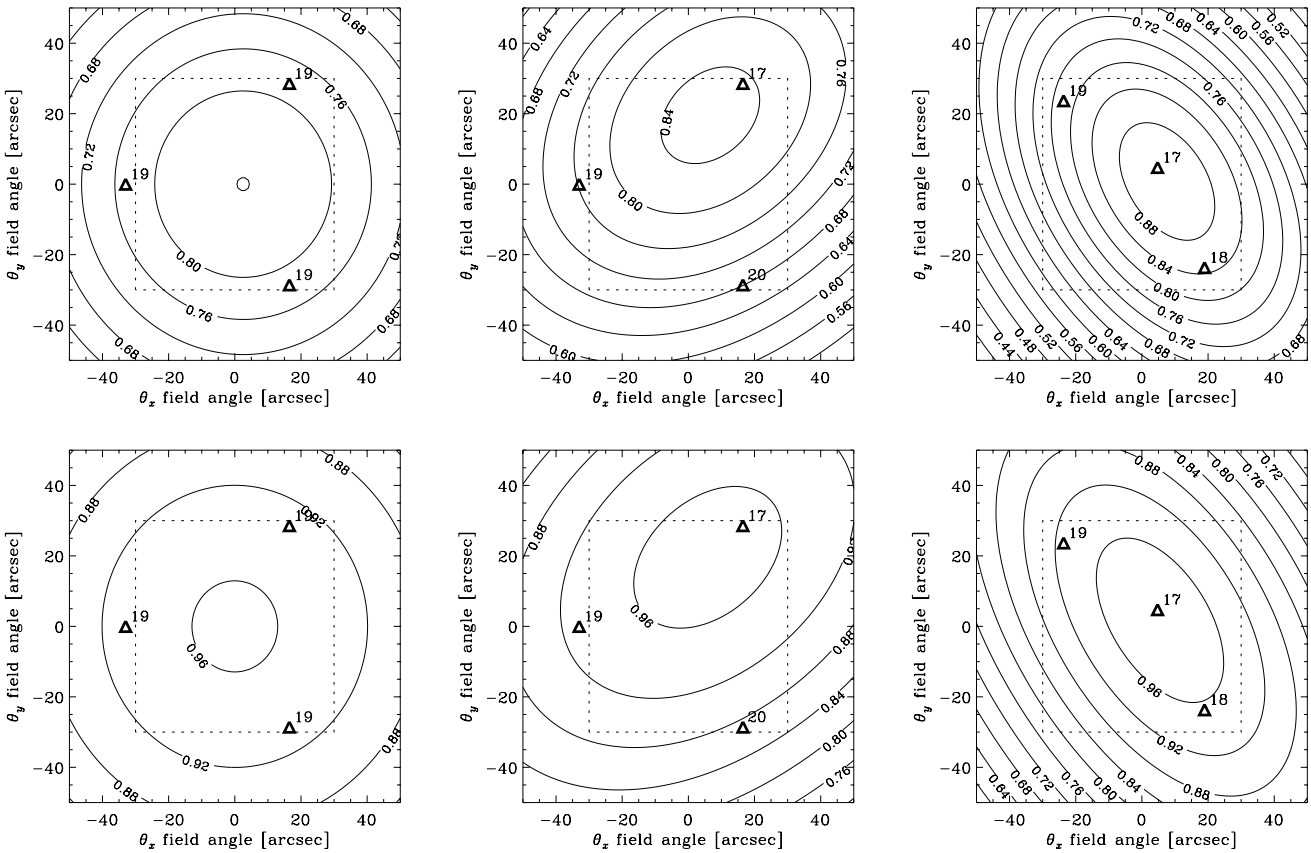


**Figure 3.** Strehl contour plots versus field angle for three sample NGS configurations with a first order integrator (top row) and the ideal predictor (top row). NGS locations are marked by triangles and their $R$ band magnitudes, and the dotted lines define the square spanned by the LGS.

Neglected in (21) is an aliasing OTF, and if the optical system suffers non-common path aberrations these may be accounted for by replacing the ideal $B_{tel}$ by a static aberration OTF. Ultimately, $B_\gamma$ will be multiplied onto the high-order OTFs to give the complete PSF reconstruction for the system.

## 6. RESULTS

The predictive form (18) of the covariance matrix $C_\gamma$, based upon *a priori* knowledge, can be evaluated numerically for a given system configuration and atmospheric turbulence profile. We have adopted the median Cerro Pachon turbulence profile (Vernin *et al.*, 2000)[7] used in Gemini MCAO simulations for the GSAO (Gemini-South Adaptive Optics) system, which is a 7-layer fit with the following altitudes, turbulence strengths and wind speeds:

$$C_n^2 \propto [0.645, 0.08, 0.12, 0.035, 0.025, 0.08, 0.015] \quad \text{normalized} \tag{25}$$

$$h = [0, 1.8, 3.3, 5.8, 7.4, 13.1, 15.8] \quad \text{km} \tag{26}$$

$$v = [6.7, 8.3, 13.4, 25.6, 33.9, 22.2, 8.9] \quad \text{m/s}. \tag{27}$$

The integrated $r_0$ at 0.5 $\mu$m is 16.6 cm, amounting to a $K$ band seeing of $0.6''$. The modal noise covariance matrix $C_n$ requires the reconstruction matrix $E$ and a statistical estimate of the noise $\sigma_m$ on the NGS tilt measurements. The present performance estimation employed the Gauss-Markov estimator

$$E_{GM} = (D^T C_n^{-1} D)^{-1} D^T C_n^{-1}, \tag{28}$$

which is a noise-weighted least-square estimator (LSE), $D$ being the interaction matrix. The virtue of the GME over the simple LSE $E_{LS} = (D^T D)^{-1} D^T$ becomes significant only in cases of severe mode degeneracy, when the NGS

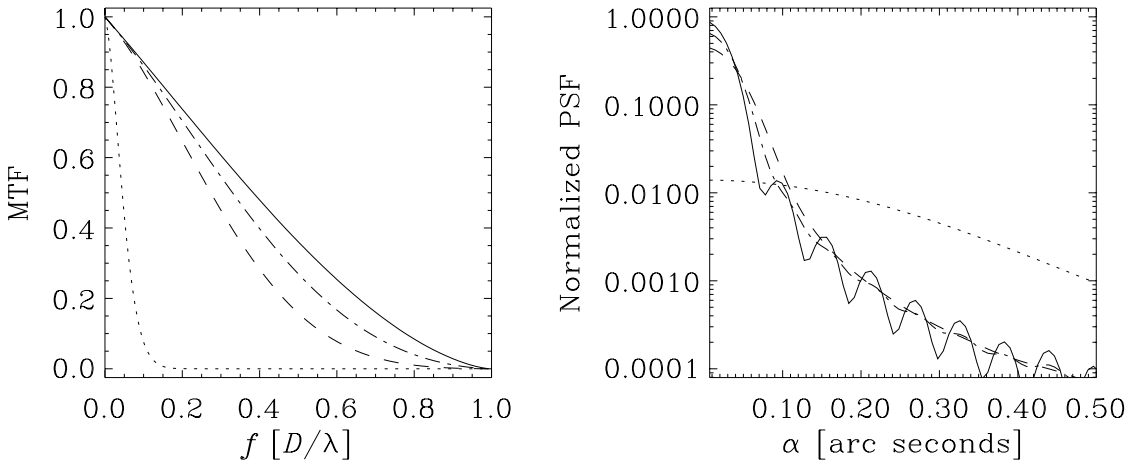


**Figure 4.** Modulation transfer functions (left) and point spread functions (right) for the asymmetric $R = [19, 17, 18]$ case in the third column of figure 3: on-axis (solid) and off-axis $(-40'', -40'')$ (dashed) with integrator controller, off-axis with predictive controller (dot-dashed), and for comparison the seeing-limited (dotted) case.

configuration is unable to uniquely determine all the null-modes (*e.g.* the NGS magnitudes differ greatly, or the NGS are nearly on a line). Since the noise $\mathbf{m}$ should not be correlated between the WFS subapertures, $\langle \mathbf{m}\mathbf{m}^T \rangle$ is diagonal with $\sigma^2_{m_i}$ on the diagonal. For a quad-cell detector, the centroid rms is equal to the spot size divided by the SNR

$$\sigma_m = \frac{\theta_B}{SNR} \approx \frac{\lambda}{r_0} \times \frac{0.587}{SNR} \quad \text{[arc seconds]}. \tag{29}$$

The performance was evaluated at pre-optimized gains, where the modal gain optimization was done in simplest possible fashion by a global downhill simplex algorithm over the five gains with the average rms wavefront for metric. As parameter space is vast, this report can only examine a few sample cases; a more complete analysis is carried out elsewhere. Figures 3 and 4 show $K$ band results for an 8-m telescope and some sample NGS configurations, with a simple integrator and a predictor. The improvement brought by the ideal temporal predictor is significant.

## 7. CONCLUSIONS

Tilt anisoplanatism is a real concern when doing tomography with LGS. It is of importance to be able to model these effects for reasons of prediction, real time compensation and post-processing such as PSF retrieval. This analysis shows that one can predict the effects of tilt anisoplanatism in an MCAO system given the geometry and magnitudes of the NGS used for tip/tilt sensing, and that a predictive temporal controller can significantly improve performance of the null-mode correction by compensating for the loop delay. The geometry of NGS are crucial to the compensation, but given an adequate configuration, the analysis shows that with a predictive controller one can use stars as faint as $R = 19$ and have nearly perfect compensation. For near-degenerate NGS configurations, brighter stars are required to obtain modal SNR and good compensation. The analysis can be extended to real-time PSF diagnostics in closed loop (in preparation), where Monte Carlo simulations are used to generate loop data as input to the algorithm.

## ACKNOWLEDGMENTS

The Gemini 8-m Telescopes Project and Observatory is managed by the Associations of Universities for Research in Astronomy, for the National Science Foundation and the Gemini Board, under an international partnership agreement. The authors would like to thank Brent Ellerbroek and Jean-Pierre Véran for useful comments and fruitful discussions.

## REFERENCES


1. F. Rigaut and E. Gendron, "Laser guide star in adaptive optics: the tilt determination problem," *Astron. Astrophys.* **261**, pp. 677–684, 1992.
2. B. Ellerbroek and T. Rhodarmer, "Adaptive wavefront control algorithms for closed loop adaptive optics," *Mathematical and Computer Modelling* **33**, pp. 145–158, 2001.
3. C. Dessenne, P.-Y. Madec, and G. Rousset, "Optimization of a predictive controller for closed-loop adaptive optics," *Appl. Opt.* **37**, pp. 4623–4633, 1998.
4. F. Roddier, M. Northcott, J. Graves, D. McKenna, and D. Roddier, "One-dimensional spectra of turbulence-induced Zernike aberrations: time-delay and isoplanicity error in partial adaptive compensation," *J. Opt. Soc. Am. A* **10**(5), pp. 957–965, 1993.
5. M. R. Whitely, M. C. Roggemann, and B. M. Welsh, "Temporal properties of the zernike expansion coefficients of turbulence-induced phase abberations for aperture and source motion," *J. Opt. Soc. Am. A* **15**(4), pp. 993–1005, 1998.
6. J.-P. Véran, F. Rigaut, H. Maître, and D. Rouan, "Estimation of the adaptive optics long exposure point spread function using control loop data," *J. Opt. Soc. Am. A* **14**(11), 1997.
7. J. Vernin, A. Agabi, R. Avila, M. Azouit, R. Conan, F. Martin, E. Masciadri, L. Sanchez, and A. Ziad, "Gemini CP Site Characterization Report," Internal report RPT-AO-G0094, Gemini Observatory, January 2000.